WOODS HOLE OCEANOGRAPHIC INSTITUTION

Reference No. 62-12

Predicting Sonic Pulse Shapes of Underwater Spark Discharges

WOODS HOLE, MASSACHUSETTS

WOODS HOLE OCEANOGRAPHIC INSTITUTION
Woods Hole, Massachusetts

Reference No. 62-12

Predicting Sonic Pulse Shapes of Underwater Spark Discharges

Also issued as WHOI CN 1270
Deep-Sea Research 1962, Vol 9. p 339-348

By

David D. Caulfield

March 1962

Submitted to Office of Naval Research under Contract Nonr 1367(00)
NR 261-103

APPROVED FOR DISTRIBUTION Paul M. Fye

Paul M. Fye, Director

ABSTRACT

Measurements of the acoustic pressure of spark discharges were made at a shallow depth (10 feet) for various voltages, stored energies, inductances and capacitances of the system, and electrode areas. The voltages ranged from 1500 V to 11 KV, and the energy storing capacitances from 8 to 800 ufd. In this range the peak pressure observed was proportional to peak current and the decay constant of the pressure-time curve was essentially the same as the electrical discharge decay constant.

TABLE OF CONTENTS

TABLE OF CONTENTS (Continued)

Section A: INTRODUCTION

High energy acoustic pulse generators are useful for studying the marine environment by sonic methods. Among the many systems that have been employed (solid and gas chemical explosives, mechanical, magnetostrictive, piezoelectric and eddy current transducers), one of the simplest is the discharge of a spark from a high energy storage capacitor bank directly into the water.

For mapping, by seismic methods, geologic structures buried beneath the ocean floor, it is often desirable to be able to control the energy vs. frequency spectrum of the sonic pulse. Sediments have attenuation factors that are frequency dependent, that is $\alpha = k f^{n}$. An extrapolation of Shumway's work indicates that n lies between 1/2 and 2 (Ref. 6). Thus, as greater penetration is required, lower frequencies must be used. However, since the ability of a sonic system to resolve range differences depends on the wavelengths being employed, it follows there will be some pulse spectrum which provides the best compromise between penetration and resolution. In order to determine the spectrum a study was made of the effects of variations in the circuit constants.

In this paper, the sparker system is described. The electrical circuit is discussed and appropriate approximations are made to aid in analysis. Various models are discussed with their related effects on the current equations. Power and energy equations are developed. The energy spectrum is obtained from the pressure-time curve by Fourier analysis.

From the above models a method for determining the initial pulse shape of the spark pressure wave is developed for use with the general values of voltages and capacitors discussed. Because considerable work has been done in the field of bubble pulse phenomena this is not covered in this report (Ref. 2). A bubble pulse does occur in spark work and, as in explosives, it is related to amount of energy in the initial disturbance, but in other respects the spark bubble pulse deviates from those of explosives.

Section B: DETERMINATION OF AN EQUIVALENT CIRCUIT REPRESENTING THE SPARKER SYSTEM

The basic sparker system used for generating underwater sonic pulses consists of energy storage unit (capacitors), switching system (ignitrons, air gap), transmission line, and electrodes and the spark (Figure 1).

The complete equivalent circuit of this system is shown in Figure 2. The equations applicable to this case are now developed and this general equivalent circuit is reduced to its most important parameters.

Some of the reactances, such as the internal inductances of the capacitors or inductance of the switching systems, are not easily calculated and were measured experimentally. For this reason the analysis of the equivalent circuit is made in several steps.

1. The equations governing LCR series discharge.

This is a straight-forward analysis of an LCR network. It is important because it is comparable to the actual storage and switch system, shorted at the output. The known quantities are the capacitance of the storage unit and the initial voltage. The problem is to obtain equations governing the current. The circuit diagram illustrating this first step is represented in Figure 3.

Let Q = Charge on the Capacitor

I = dQ/dt with initial conditions Qo = Initial Charge = CV_o

V_o = Initial Voltage

$$\left.\frac{dQ(t)}{dt}\right|_{t=0} = I_o = 0.$$

General Equation:

$$L\frac{d^2Q(t)}{dt^2} + R\frac{dQ(t)}{dt} + \frac{1}{C}Q(t) = 0.$$

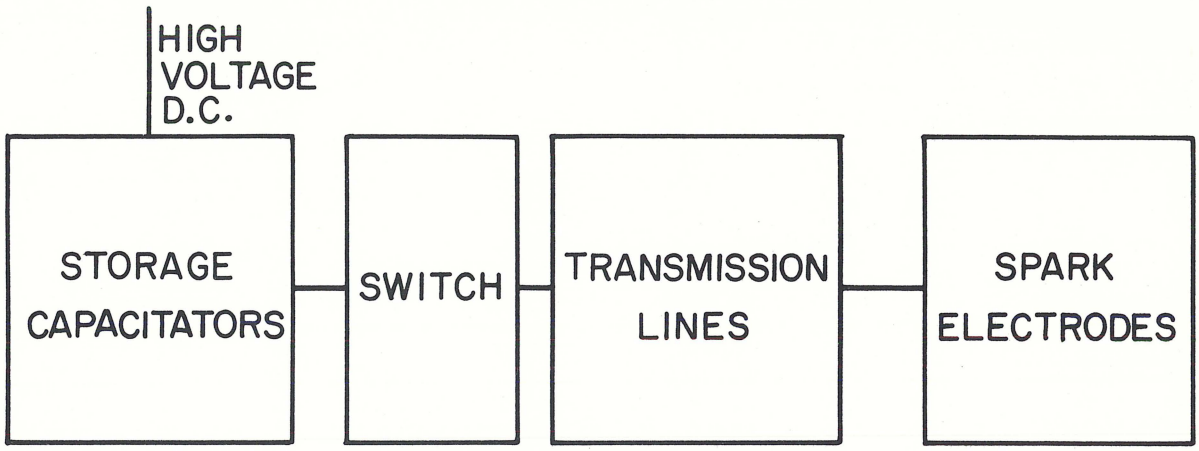

BLOCK DIAGRAM

FIGURE 1

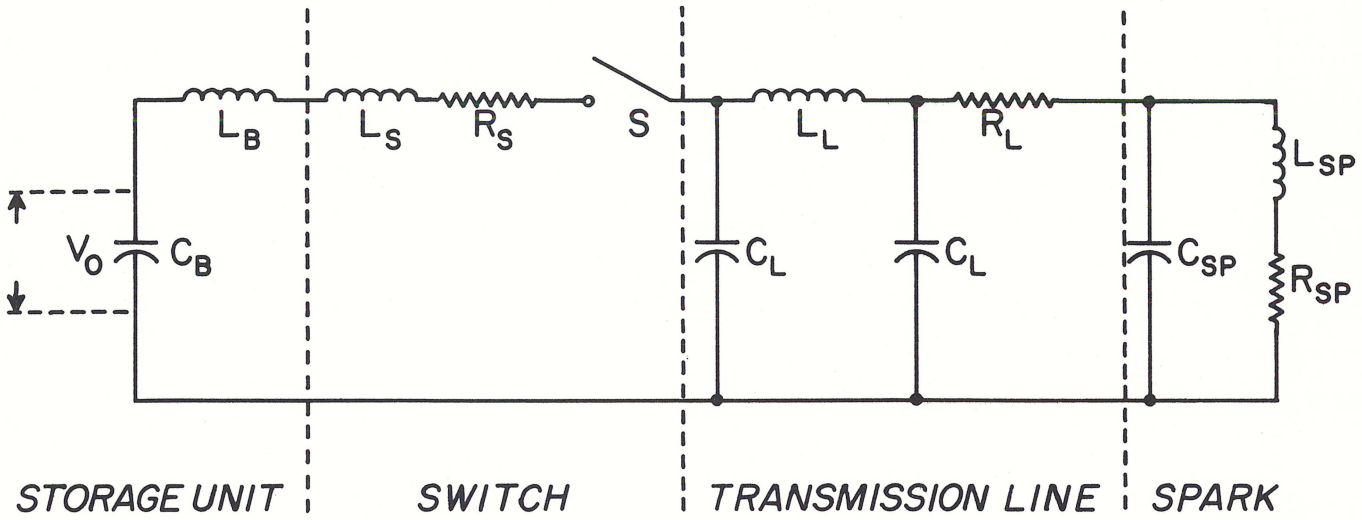

C_L = TRANSMISSION LINE CAPACITANCE
L_L = INDUCTANCE OF TRANSMISSION LINE
R_L = RESISTANCE OF LINE
L_{SP}= INDUCTANCE OF SPARK
R_{SP}= RESISTANCE OF SPARK
C_{SP}= CAPACITANCE OF SPARK
V_O = INITIAL VOLTAGE ON BANK
C_B = CAPACITANCE OF STORAGE UNIT
L_B = INDUCTANCE OF BANK
R_S = RESISTANCE OF BANK AND SWITCH
S = SWITCH
L_S = INDUCTANCE OF SWITCH

COMPLETE EQUIVALENT CIRCUIT

FIGURE 2

Solving this Equation yields:

$$Q(t) = -Q_0 e^{-bt} \cos \omega t - \frac{1}{\omega} Q_0 b e^{-bt} \sin \omega t \quad (2)$$

Where $b = R/2L$ (3)

and $\omega = \sqrt{1/CL^2 - R^2/4L^2}$ (4)

Noting that $I = dQ/dt$ and applying the initial conditions on this equation, we obtain the equation for the current.

$$I = \frac{V_0}{\omega L} e^{-bt} \sin \omega t \quad (5)$$

With b and ω given by (3) and (4) respectively, as above.

2. Determination of the damping factor, R/2L.

One of the problems of the analysis is that of determining the R and L constants of the circuit. These quantities are determined by measuring the logarithmic decrement, which is defined as the natural logarithm of the ratio of any two successive amplitudes of a decaying oscillatory wave.

Looking at the general equation of current:

$$I = \frac{V_0}{L\omega} e^{-bt} \sin \omega t \quad (5)$$

it is noted that when $\sin \omega t = 1$, the curve is tangent to the exponential envelope Xe^{-bt}. The tangents are not horizontal but can be taken as such for a first approximation (Figure 4).

The logarithmic decrement δ is then defined as:

$$\delta = \ln \frac{X_1}{X_2} = \ln \frac{e^{-bt_1}}{e^{-b(t_1+\tau)}} = \ln e^{b\tau} \quad (6)$$

where τ is the period of the sine function.

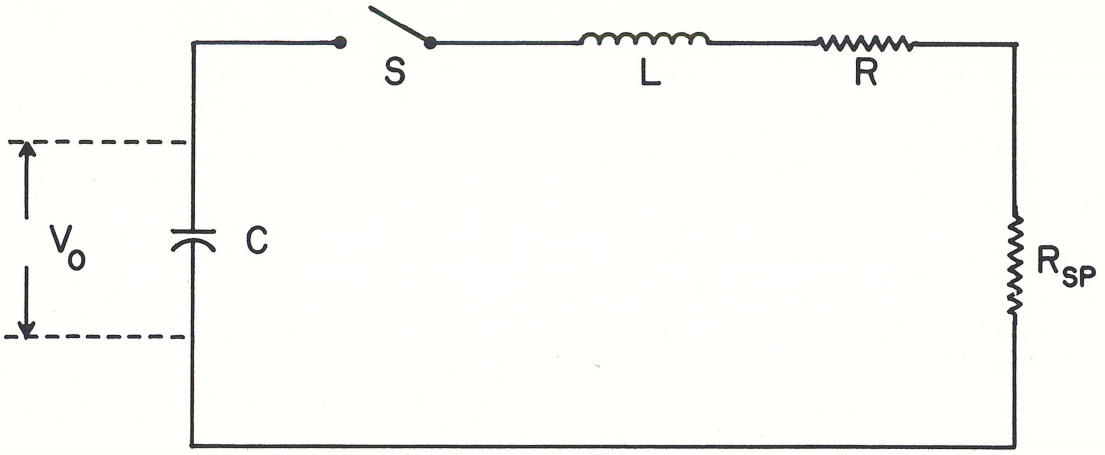

C = CAPACITANCE STORAGE SYSTEM
L = TOTAL INDUCTANCE OF SYSTEM
$(L_B + L_S + L_L)$
R = TOTAL CIRCUIT RESISTANCE $(R_S + R_L)$
R_{SP} = SPARK RESISTANCE
S = SWITCH

A TYPICAL CIRCUIT

FIGURE 3

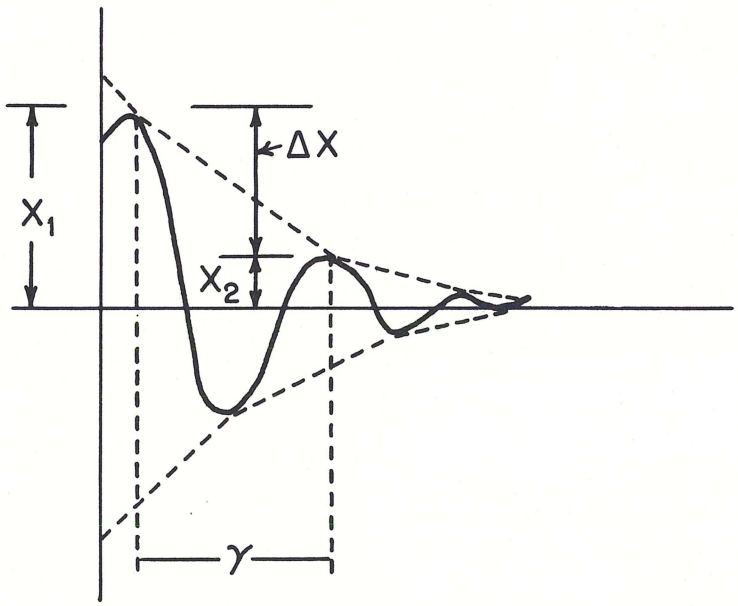

TYPICAL OSCILLATORY WAVE PATTERN FROM A SHORTED STORAGE BANK

FIGURE 4

We can use this formula to determine b from any of the voltage and current measurements. Therefore substituting equation (6) into equation (4) we have:

$$\omega = \sqrt{1/CL - b^2} \qquad (7)$$

Since we know ω and C for a particular case, we can solve for L (inductance) and then for R (resistance).

3. Transmission Line Representation.

Figure 5 shows the usual representation of a transmission line. The capacitances, C_L, complicate the system; let us examine the justification for neglecting them. It is known that we are primarily interested in the acoustic range of frequency (i. e. 20 cps to 30 kc). From our experiments we know that the range of frequency of the electrical signals is also in this range, hence we can compute an order of magnitude for one wave-length of signal. The phase velocity for the cables commonly employed in spark power transmission is around 6000 ft/10^{-5} sec. (Ref. 7), therefore, one wave-length is much longer than any length of cable employed making the voltage/current ratio = (E/I) constant along the line. A constant E/I ratio means that the internal capacitance of the transmission line C_L can be neglected. See Figure 6 for the new representation which is an inductance and a resistance in series.

4. Approximation of Spark Impedance.

The circuit representation and physical layout of the spark electrode system is shown in Figure 7. The spark occurs at the small center electrode. Some approximations can be made from the physical layout of the spark electrodes. The size of the electrode is small compared with the length of the transmission line and the geometry of construction is usually coaxial or cylindrical, hence we can make the assumption that the inductance and capacitance associated with the spark electrode are negligible compared to the rest of the system. Also the experimental results show that the equivalent inductance and capacitance of the spark discharge are small compared with the inductance and capacitance of the system, and that the resistance of the spark stays relatively constant. This means that we can represent the spark by a resistance.

5. Summary of Section 1.

We have now discussed all the components that make up the sparker system and what assumptions can be made about each. These components are

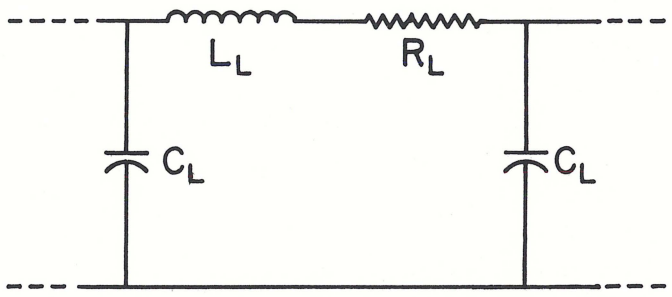

C_L = TRANSMISSION LINE CAPACITANCE
L_L = " " INDUCTANCE
R_L = " " RESISTANCE

USUAL TRANSMISSION LINE REPRESENTATION

FIGURE 5

L_L = TRANSMISSION LINE INDUCTANCE
R_L = " " RESISTANCE

NEW REPRESENTATION OF TRANSMISSION LINE

FIGURE 6

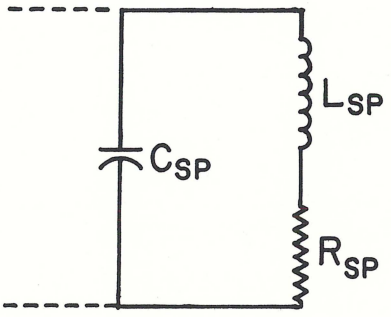

C_{SP} = SPARK CAPACITANCE
L_{SP} = " INDUCTANCE
R_{SP} = " RESISTANCE

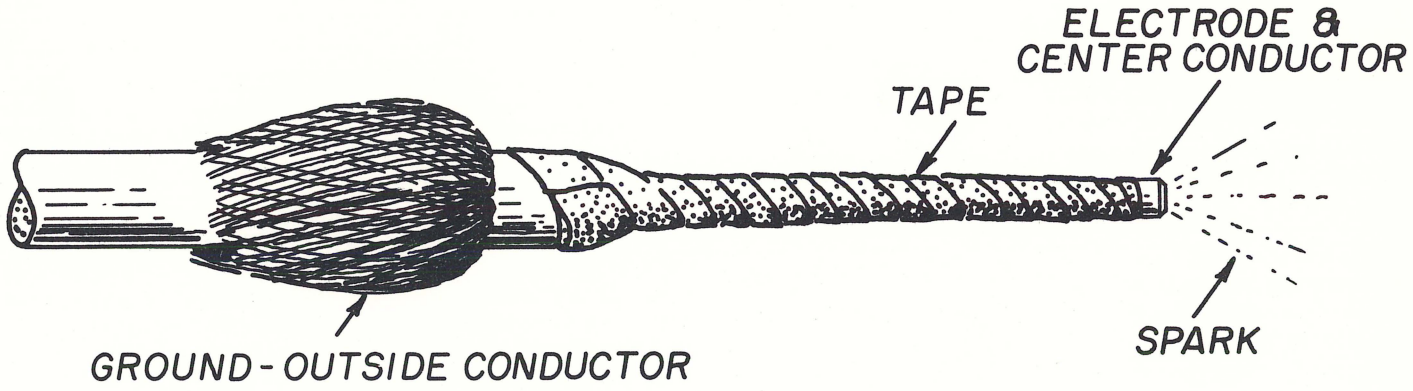

SPARK ELECTRODE CONFIGURATION

FIGURE 7

combined into a simplified equivalent circuit. Figure 8 shows these reduced into four general parts, which are combined into an LCR series circuit to which the equations for current developed in Step 1 are applicable. The current in this circuit may be oscillatory, critically damped, or overdamped, depending on the circuit constants.

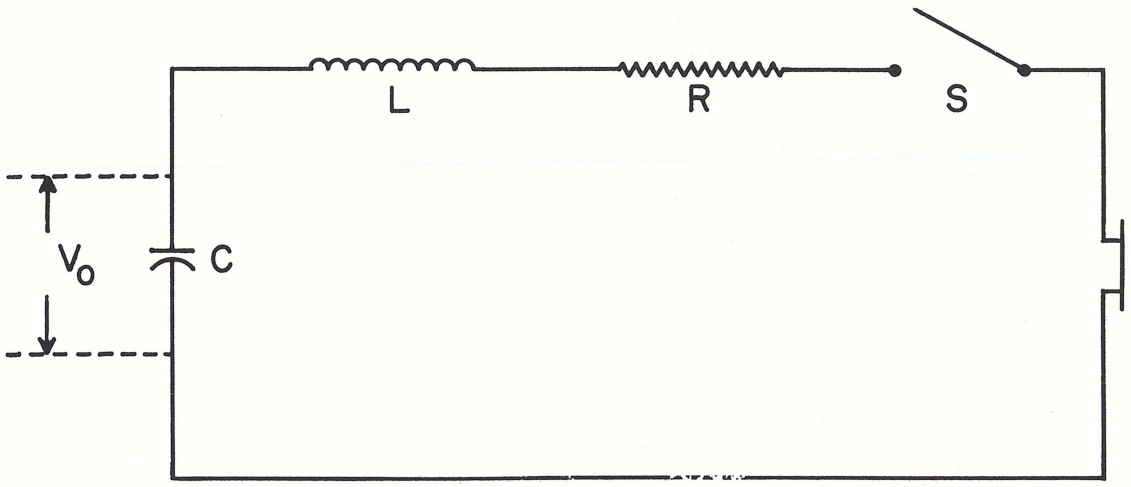

C = CAPACITANCE
L = INDUCTANCE
R = RESISTANCE
V_o = INITIAL VOLTAGE

REDUCED GENERAL CIRCUIT

FIGURE 8

Section C: DETERMINATION OF PEAK CURRENT, TOTAL POWER, AND ENERGY DELIVERED TO SPARK

1. For an oscillatory current

The general equation for current flow is developed in Section B, Step 1.

$$I = \frac{V_o}{L\omega} e^{-bt} \sin \omega t. \qquad (5)$$

At the peak current the time derivative (dI/dt) equals zero. Therefore differentiation of equation 5 with respect to time, setting equal to zero and solving for time,

$$t_{max} = \frac{1}{\omega} \arctan \omega/b, \qquad b = R/2L \quad \omega = 2\pi f. \qquad (8)$$

Substituting equation 8 into the current equation gives the peak current:

$$I_{max} = \frac{V_o}{L\omega} e^{-\frac{b}{\omega} \arctan \omega/b} \sin[\arctan \omega/b]. \qquad (9)$$

This equation is later used to calculate the peak current from the initial conditions enabling one to relate calculated peak current and measured peak pressure.

In determining the power delivered to the spark we note that

$$\text{Power} = P = R_{sp} I^2. \qquad (10)$$

We know both the quantities R_{sp} = Spark Resistance and I; hence it is possible to express the power as a function of time,

$$P = R_{sp} \left(\frac{V_o}{L\omega}\right)^2 e^{-2bt} \sin^2 \omega t. \qquad (11)$$

and the total energy is the integral of this equation over time.

$$E_{TOTAL} = R_{sp} B^2 \int_0^\infty e^{-2bt} \sin^2 \omega t \, dt, \quad B = \frac{V_o}{L\omega}. \qquad (12)$$

Evaluating this integral, we have:

$$E_{TOTAL} = R_{sp} B^2 \frac{\omega^2}{b(b^2+\omega^2)}. \qquad (13)$$

This is the energy delivered to the spark.

2. For an overdamped current.

As the value of the capacitance in the storage unit is made larger, and/or if the inductance of the system is made smaller,

$$\omega = \sqrt{1/LC - R^2/4L^2} \qquad (4)$$

becomes imaginary, and the current equation is better expressed as:

$$I = B e^{-bt} \sinh kt \qquad (14)$$

$$K = \sqrt{R^2/4L^2 - 1/LC}, \quad b = R/2L$$

$$B = V_0/KL, \quad V_0 = \text{Initial Voltage}.$$

An exponential form of this equation is more convenient:

$$I = B/2 \left(e^{-(b-k)t} - e^{-(b+k)t} \right) \qquad (15)$$

The equations expressing the time to reach peak current, and the value of peak current are:

$$t_{max} = \ln \left(\frac{b-k}{b+k} \right)^{1/2k} \qquad (16)$$

$$\text{and} \quad I_{max} = B/2 \left[e^{-(b-k)\ln\left(\frac{b-k}{b+k}\right)^{\frac{1}{2}k}} - e^{-(b+k)\ln\left(\frac{b-k}{b+k}\right)^{\frac{1}{2}k}} \right] \qquad (17)$$

For this case the total energy to the spark is

$$E_{TOTAL} = R_{sp} B^2/4 \int_0^\infty \left[e^{-(b-k)t} - e^{-(k+b)t} \right]^2 dt \qquad (18)$$

$$= R_{sp} B^2/2b \left(\frac{k^2}{b^2 - k^2} \right) \qquad (19)$$

Section D: THE ENERGY SPECTRUM OF THE INITIAL PRESSURE WAVE RESULTING FROM THE SPARK DISCHARGE

Since we have the pressure as a function of time (measured experimentally), it is desirous to know the energy spectrum of the initial pressure pulse. This problem can be simply solved, to a first approximation, if we assume that the pressure time curve is a decaying exponential function (i. e. neglecting finite initial rise time).

The equation approximating the first pressure pulse as a function of time is:

$$p = p_0 e^{-mt} \qquad (20)$$

where p = pressure ($dyne/cm^2$),
p_0 = peak pressure ($dyne/cm^2$ at 1 meter),
and m = decay constant.

Now the acoustic energy is expressed as:

$$E = 1/\rho c \int_0^\infty |f(t)|^2 dt \qquad (21)$$

where $f(t) = p_0 e^{-mt}$, ρ = density (gm/cm^3),
and c = velocity of propagation in the medium.

The total energy may also be represented in terms of the Fourier Transforms of the pressure pulse, and hence we may obtain the energy spectrum as a function of frequency:

$$\mathcal{E}(f) = \frac{2p_0^2}{\rho c}\left(\frac{1}{m^2 + (2\pi f)^2}\right), \quad f = \text{frequency}. \qquad (22)$$

The energy $\mathcal{E}$ is expressed in energy per cycle per unit area, provided that is measured at one meter. This equation is used to plot the energy spectrum of the initial pressure pulse from the sparker, giving a method of evaluating the output of different sparker systems.

The problem of obtaining the energy spectrum has been reduced to finding the peak pressure and the decay constant. The following discussion shows how these factors are determined from the electrical constants and the experimental data.

Section E: EXPERIMENTAL SETUP

The data-taking equipment is shown in Figure 9. The position of the spark and of the measuring hydrophone (depth and separation) was held constant by an aluminum form suspended from a wooden float. The same measuring equipment was used for all experiments. The pressure transducer was a BC-32, #120, which was calibrated, with the extra length of cable attached, by Underwater Sound Reference Laboratory in Orlando, Florida (Office of Naval Research).

The spark electrode configuration was always a small center electrode where the spark occurs, and a large ground electrode (Figure 7). The field configuration is such that at the small center electrode there is a high intensity electric field, causing the breakdown to occur there. It turns out that for any given storage system and initial voltage, there is an optimum cross-sectional area of the center electrode. When the area is too large, the electric field intensity is too small, reducing breakdown, and hence peak pressure. When the area is too small the total number of particles that could have been ionized decreases; hence the system becomes inefficient. The only way found to date for determining the cross-sectional area is by experimentation.

The following units were tested with a large range of transmission lines employed to vary the inductance:

a) 8 microfarads 1-10 kv Ref. 8
b) 16 microfarads 1-10 kv Ref. 8
c) 160 microfarads 1-4 kv Ref. 9
d) 460 microfarads 1-4 kv Ref. 9

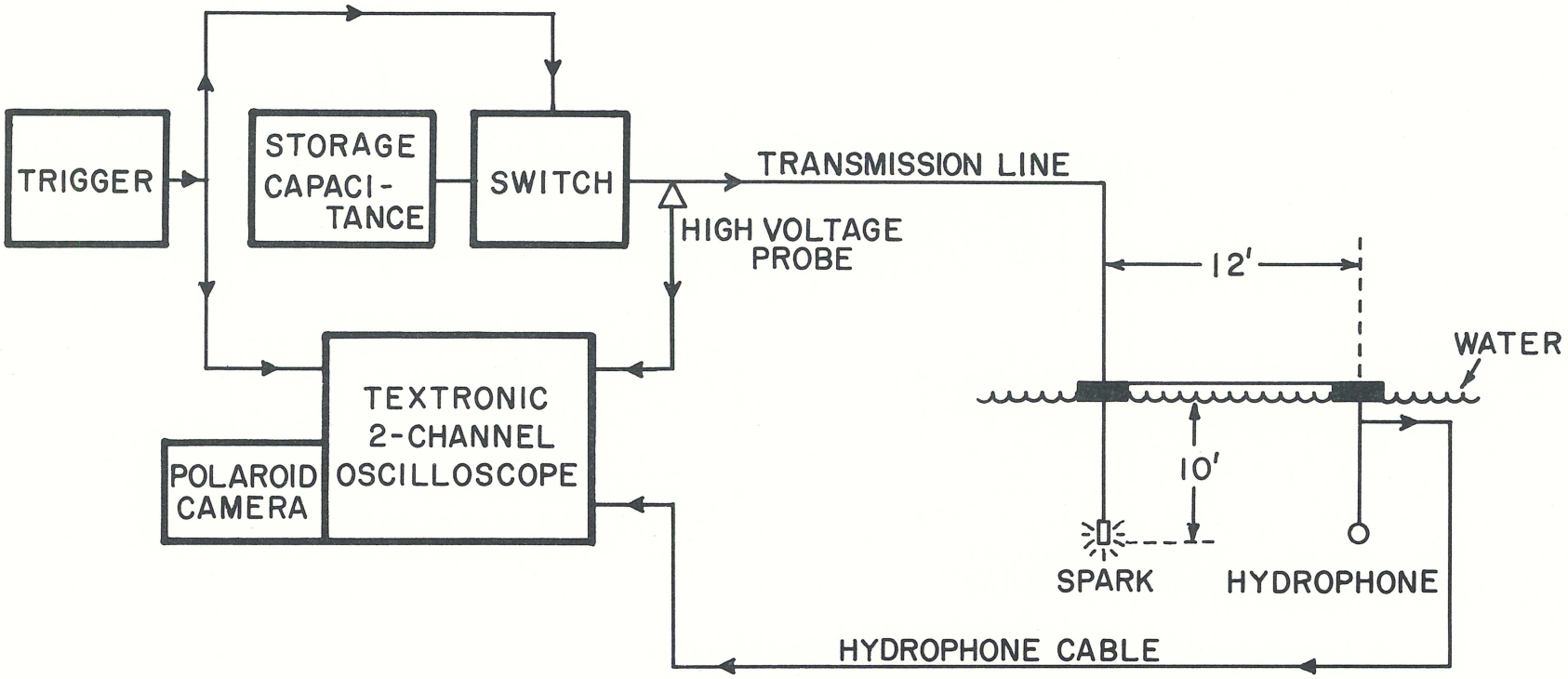

EXPERIMENTAL SETUP

FIGURE 9

Section F: SUMMARY OF CHANGES IN OUTPUT DUE TO CHANGES IN SYSTEM CONSTANTS

1. Inductance.

The major inductance in the system is in the transmission line. Changes made in this inductance by changing length, cable type, cable arrangement and number of cables resulted in increased peak pressure with reduction of inductance. A corresponding increase in peak current was also observed. The change in resistance of the lines does have some effect on peak current, but the comparison of cable arrangements of different resistance and inductance showed the inductance to be the controlling parameter. Cables were used from 200 to 1500 feet in length, with up to four cables in parallel.

2. Capacitance.

While the capacitance was varied from 8 ufd to 500 ufd (keeping the voltage and other quantities constant) the peak current and pressures remained almost constant, with the same rise time. The decay of the pressure and the current could be approximated by the equation $\psi = \psi_0 e^{-mt}$ where the decay constant m was inversely proportional to the capacitance used.

3. Variation of voltage on the storage bank.

For any given system the peak pressure and current varies linearly with the voltage across the storage capacitors (Figure 10a). This voltage has to be above a certain value for the breakdown to occur and depends on the cross-sectional area of the electrodes.

4. Variation in electrode configuration.

With a given system, that is, cable, switch and capacitors, operating at a given voltage, the size, geometry and number of electrodes influence the sonic output. With a large smooth surface exposed, no breakdown occurs. As the area is decreased, the initial electric field increases and eventually breakdown will occur when the voltage is applied. In these observations a single discharge electrode (as shown in Figure 7) was used. The area chosen was a compromise between output and life. The area was approximately 0.5 sq. inches but was varied with different systems.

For this particular geometry, it was found by measuring the logarithmic decrement that the spark resistance was 1.05 ohms; by means of the

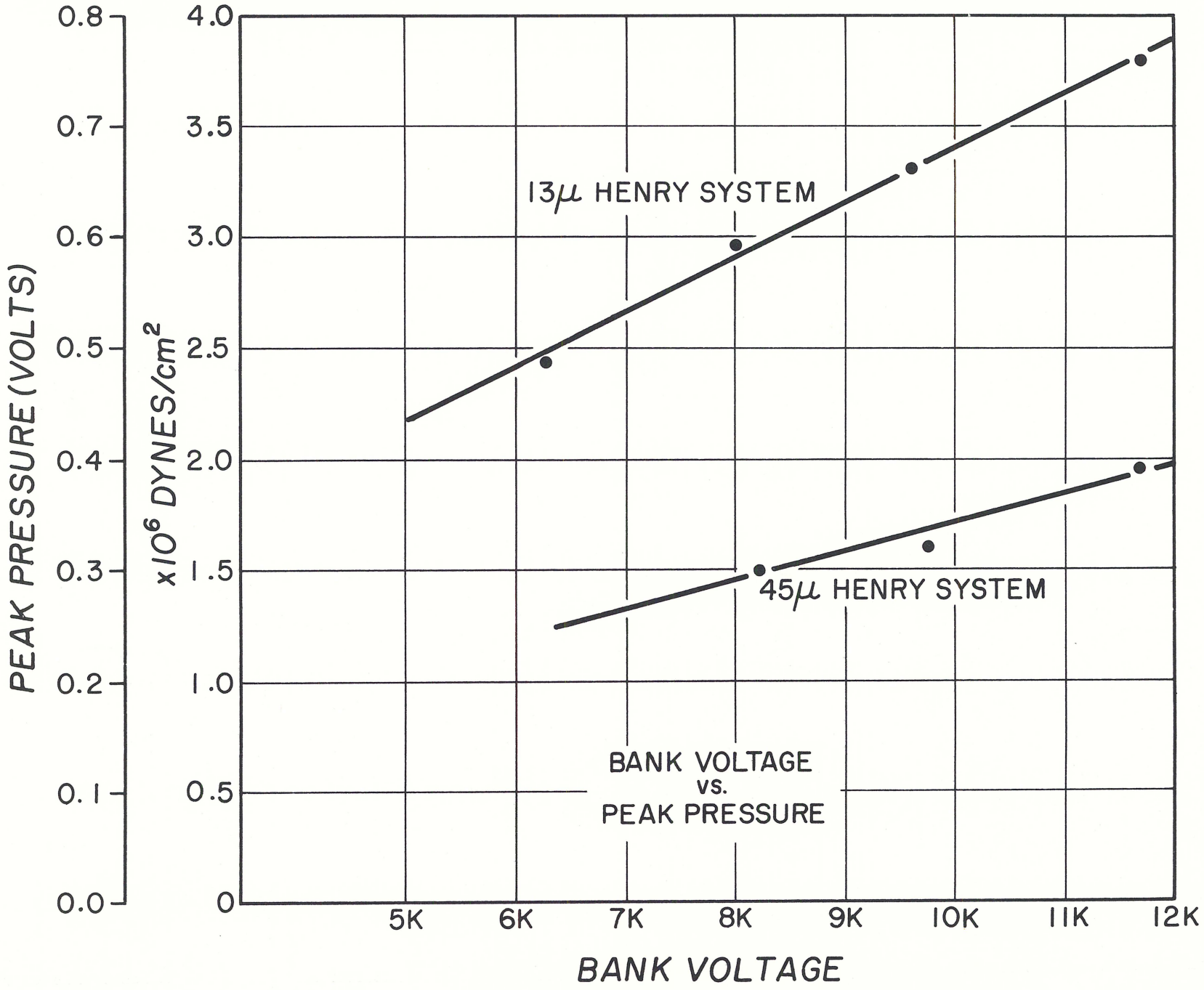
PEAK PRESSURE (VOLTS)
0.8
0.7
0.6
0.5
0.4
0.3
0.2
0.1
0.0
x10⁶ DYNES/cm²
4.0
3.5
3.0
2.5
2.0
1.5
1.0
0.5
0
13μ HENRY SYSTEM
45μ HENRY SYSTEM
BANK VOLTAGE
vs.
PEAK PRESSURE
5K
6K
7K
8K
9K
10K
11K
12K
BANK VOLTAGE

FIGURE 10a

ringing time of the circuit, the resistance was 1.15 ohms. In general, the spark resistance averaged between 1.0 to 1.2 ohms. It should be pointed out that the resistance varies as a function of time (approximately ±10%) about the value of 1.10 ohms, but we have assumed that it is constant at 1.10 ohms.

Section G: EXPERIMENTAL OBSERVATIONS OF SPECIAL INTEREST

Figure 10b is a plot of peak pressure versus peak current for different systems (changes in inductance, capacitance, voltage) with the same polarity of center electrode. In these measurements the cross-sectional area of the electrode was near optimum for each system. It is seen that all measurements are within 10% of a straight line, which is assumed to represent the linear relation between peak current and pressure.

With the simple electrode used it was observed that the polarity of the discharge electrode affected the output in peak pressure and energy. The peak pressure and energy is larger when the center electrode is positive. The increase of both of these factors is by a factor of two roughly. This increase in pressure and energy is undoubtedly due to hydrogen formation at the center electrode rather than to oxygen formation (Ref. 1).

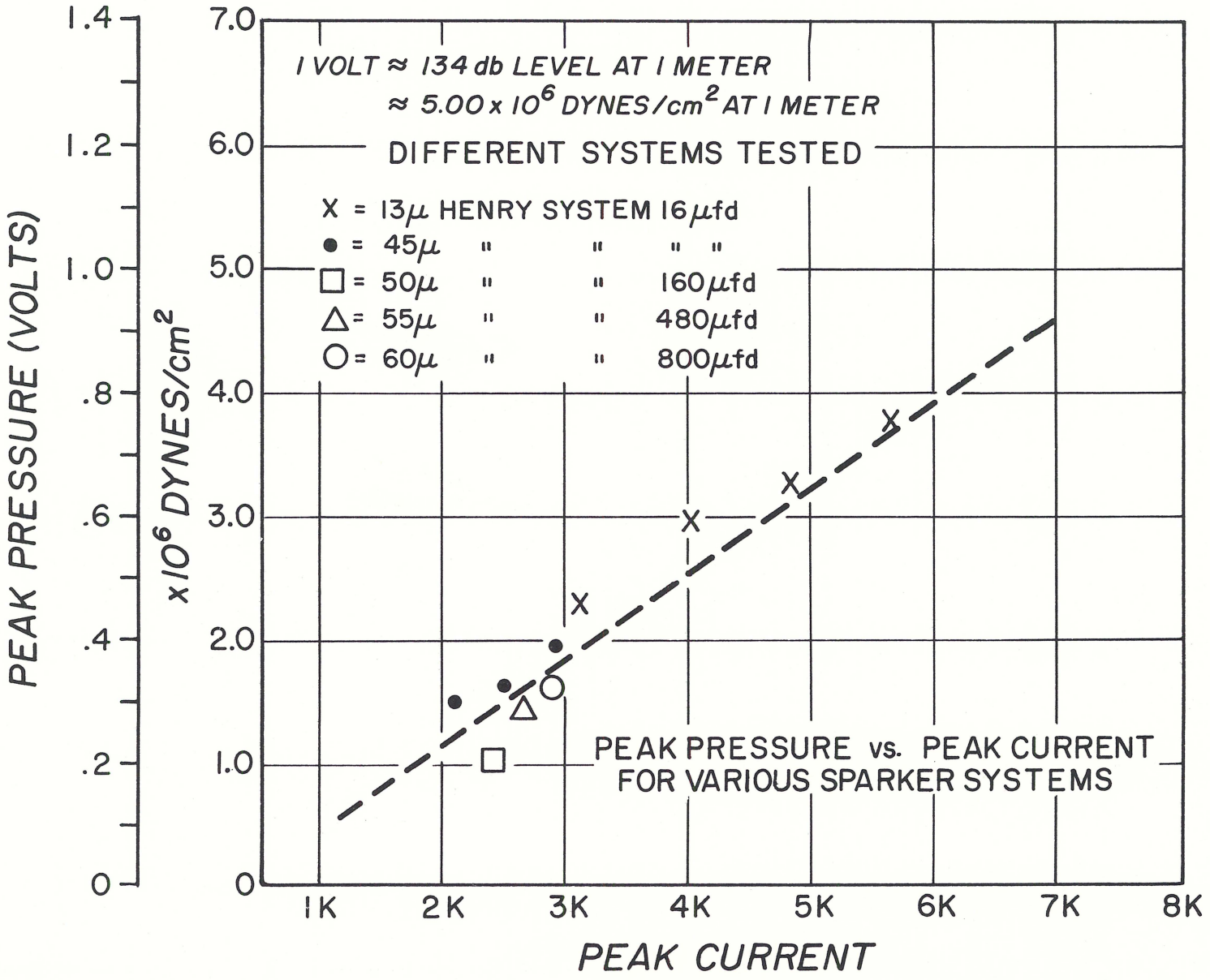
1 VOLT ≈ 134 db LEVEL AT 1 METER
≈ 5.00 x 10^6 DYNES/cm^2 AT 1 METER
DIFFERENT SYSTEMS TESTED
X = 13μ HENRY SYSTEM 16μfd
● = 45μ " " " "
□ = 50μ " " 160μfd
△ = 55μ " " 480μfd
○ = 60μ " " 800μfd
PEAK PRESSURE vs. PEAK CURRENT
FOR VARIOUS SPARKER SYSTEMS
PEAK PRESSURE (VOLTS)
x10^6 DYNES/cm^2
PEAK CURRENT
1.4
1.2
1.0
.8
.6
.4
.2
0
7.0
6.0
5.0
4.0
3.0
2.0
1.0
0
1K
2K
3K
4K
5K
6K
7K
8K

FIGURE 10b

Section H: PREDICTING THE ENERGY SPECTRUM OF A SYSTEM

The current and pressure decay curves are approximately exponential curves (Figures 11a, 11b, 12a, and 12b). When plotted as normalized magnitude versus time (Figures 11a and 11b) the curves seem different, but the decay constants in all cases for current and pressure were within 10% of each other for each sparker system.

The energy spectrum as derived in Section 3 for an exponential curve is

$$\mathcal{E}(f) = \frac{2P_0^2}{\rho c}\left(\frac{1}{m^2 + (2\pi f)^2}\right)$$

From the above equation we may obtain the form

$$\frac{dE}{E} = -\frac{2\frac{dm}{m}}{1 + \left(\frac{2\pi f}{m}\right)^2}$$

which is a fair approximation for $\Delta m = 0.1$. m in the cases studied was of the order of 1000/sec. The error in predicting the energy spectrum levels is equal to or less than 20%, with the largest value holding only for low frequencies, that is, where $2\pi f < m$. ($f \approx$ 160 c/sec).

From an engineering standpoint we can now predict the energy spectrum from the electrical parameters of the spark system if we stay within the restrictions of our simple electrode structure and the optimum exposed area of electrode.

Two examples of predicted energy spectrum are given in Figure 13. These correspond to the pressure and current curves given in Figures 11 and 12.

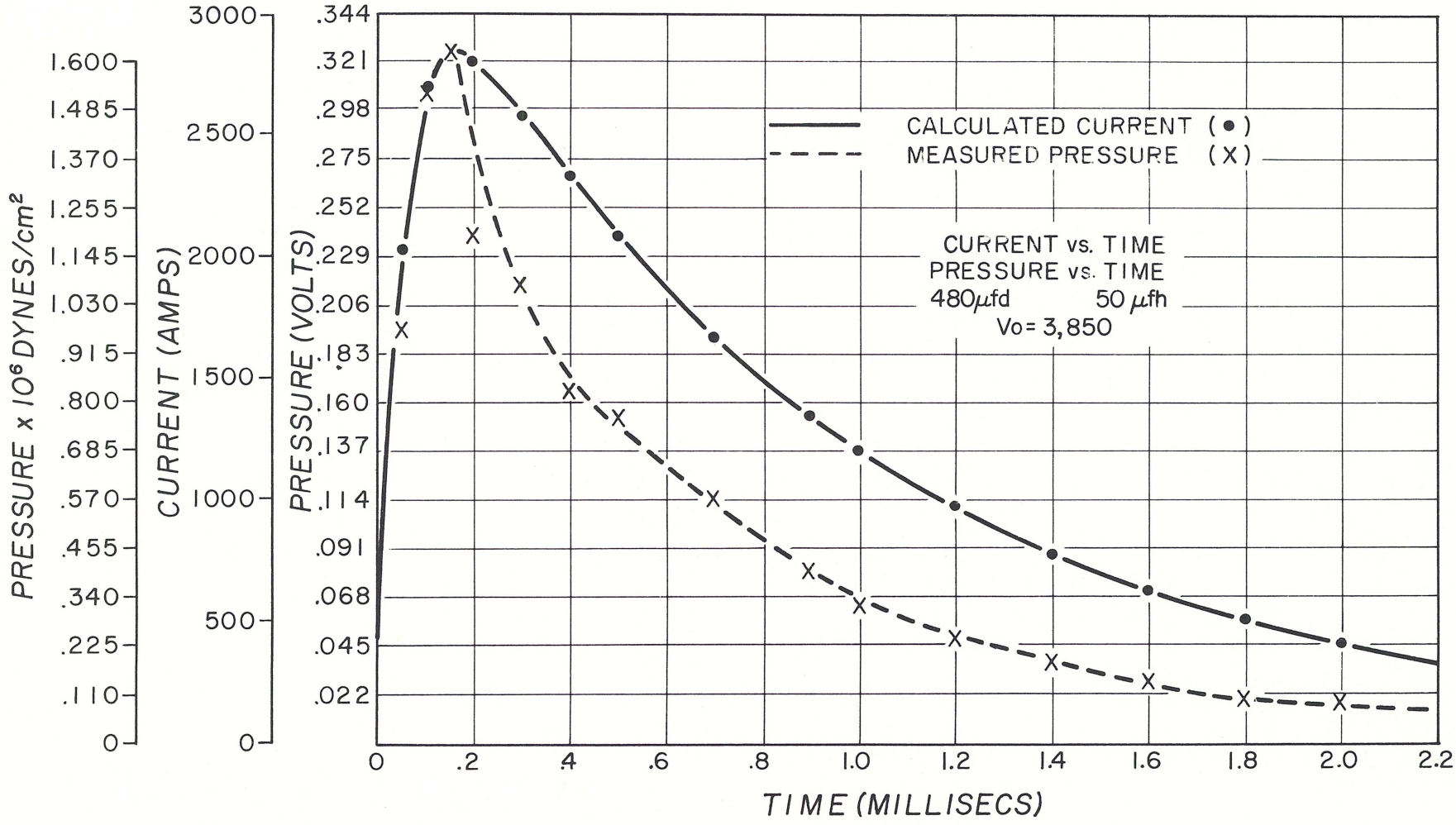
PRESSURE x 10⁶ DYNES/cm²
1.600
1.485
1.370
1.255
1.145
1.030
.915
.800
.685
.570
.455
.340
.225
.110
0
CURRENT (AMPS)
3000
2500
2000
1500
1000
500
0
PRESSURE (VOLTS)
.344
.321
.298
.275
.252
.229
.206
.183
.160
.137
.114
.091
.068
.045
.022
CALCULATED CURRENT (●)
MEASURED PRESSURE (X)
CURRENT vs. TIME
PRESSURE vs. TIME
480μfd 50 μfh
Vo = 3,850
0
.2
.4
.6
.8
1.0
1.2
1.4
1.6
1.8
2.0
2.2
TIME (MILLISECS)

FIGURE 11a

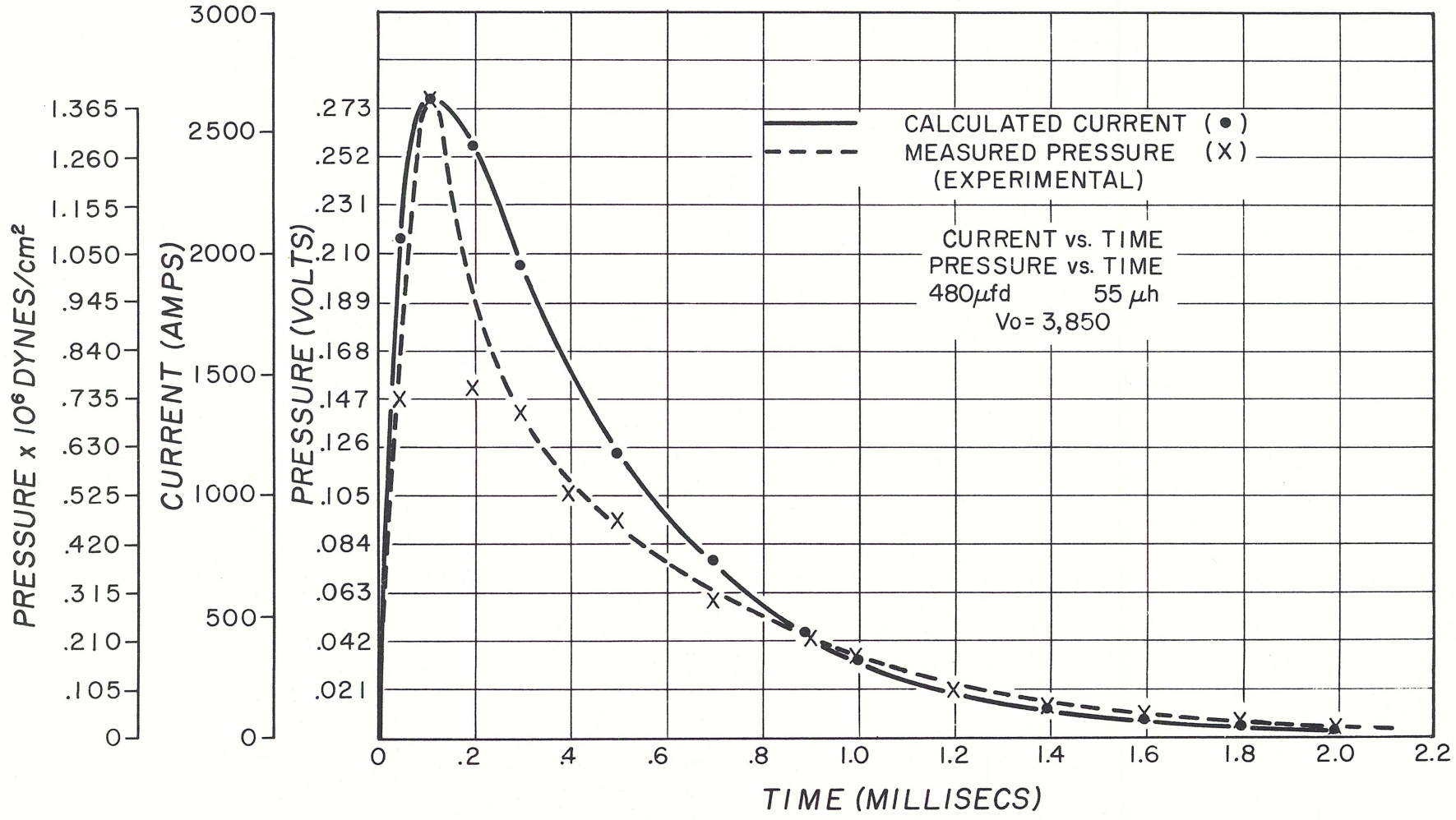
PRESSURE x 10⁶ DYNES/cm²
1.365
1.260
1.155
1.050
.945
.840
.735
.630
.525
.420
.315
.210
.105
0
CURRENT (AMPS)
3000
2500
2000
1500
1000
500
0
PRESSURE (VOLTS)
.273
.252
.231
.210
.189
.168
.147
.126
.105
.084
.063
.042
.021
CALCULATED CURRENT (●)
MEASURED PRESSURE (X)
(EXPERIMENTAL)
CURRENT vs. TIME
PRESSURE vs. TIME
480μfd 55 μh
Vo= 3,850
0
.2
.4
.6
.8
1.0
1.2
1.4
1.6
1.8
2.0
2.2
TIME (MILLISECS)

FIGURE 11b

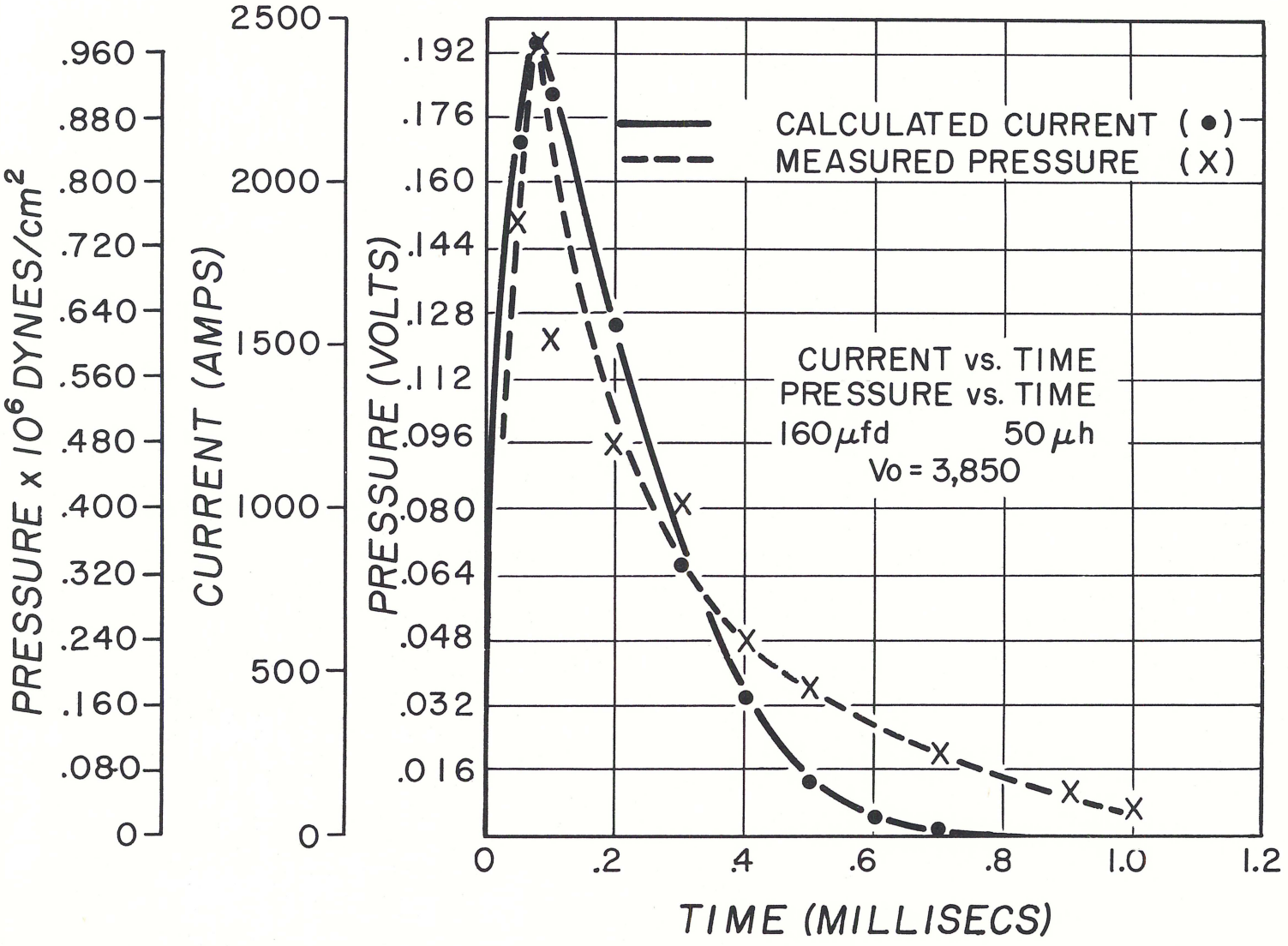
PRESSURE x 10^6 DYNES/cm^2
.960
.880
.800
.720
.640
.560
.480
.400
.320
.240
.160
.080
0
CURRENT (AMPS)
2500
2000
1500
1000
500
0
PRESSURE (VOLTS)
.192
.176
.160
.144
.128
.112
.096
.080
.064
.048
.032
.016
CALCULATED CURRENT (•)
MEASURED PRESSURE (X)
CURRENT vs. TIME
PRESSURE vs. TIME
160 μfd 50 μh
Vo = 3,850
0
.2
.4
.6
.8
1.0
1.2
TIME (MILLISECS)

FIGURE 11c

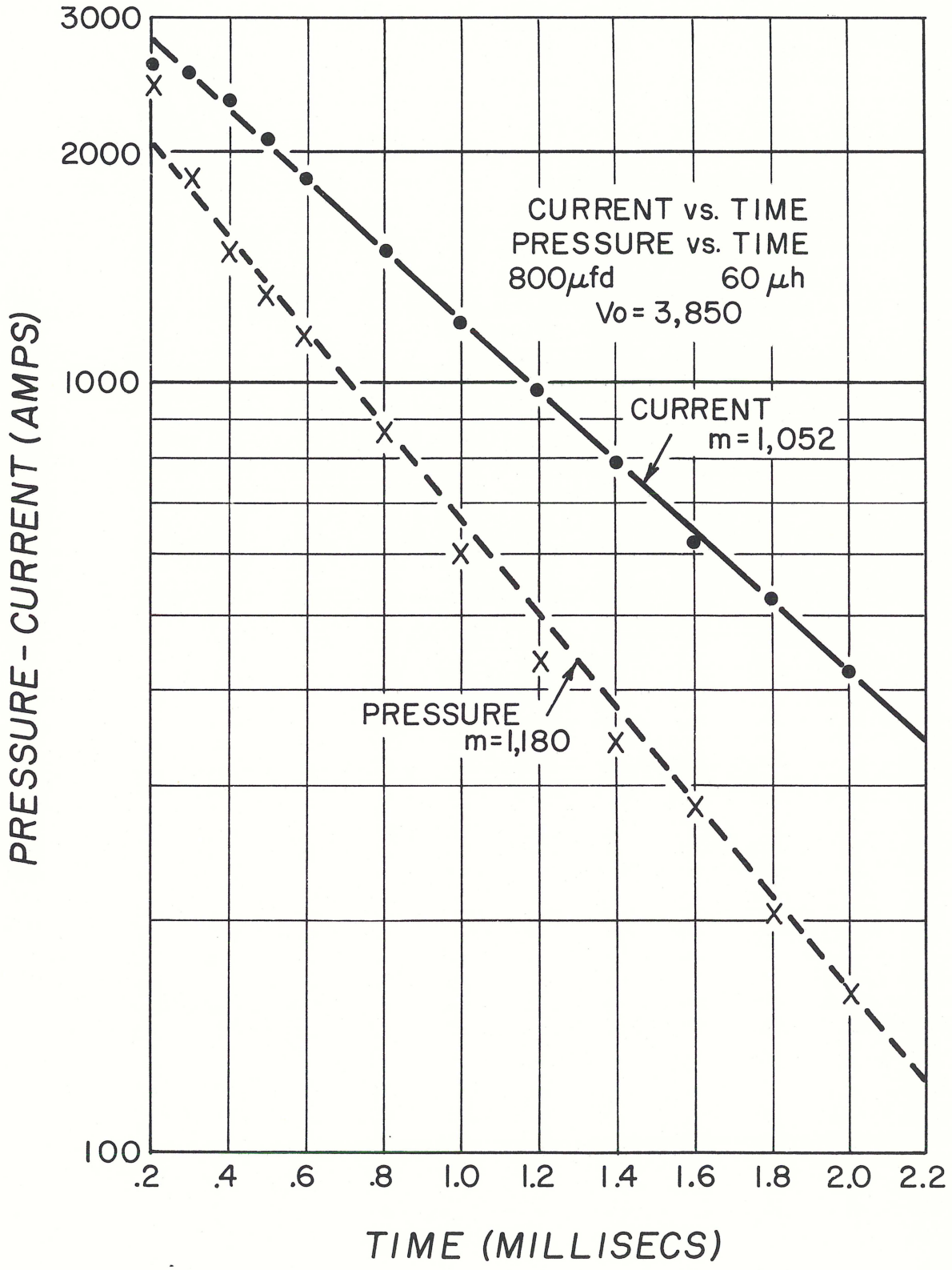
3000
2000
1000
100
.2
.4
.6
.8
1.0
1.2
1.4
1.6
1.8
2.0
2.2
PRESSURE-CURRENT (AMPS)
TIME (MILLISECS)
CURRENT vs. TIME
PRESSURE vs. TIME
800μfd 60 μh
Vo = 3,850
CURRENT
m = 1,052
PRESSURE
m = 1,180

FIGURE 12a

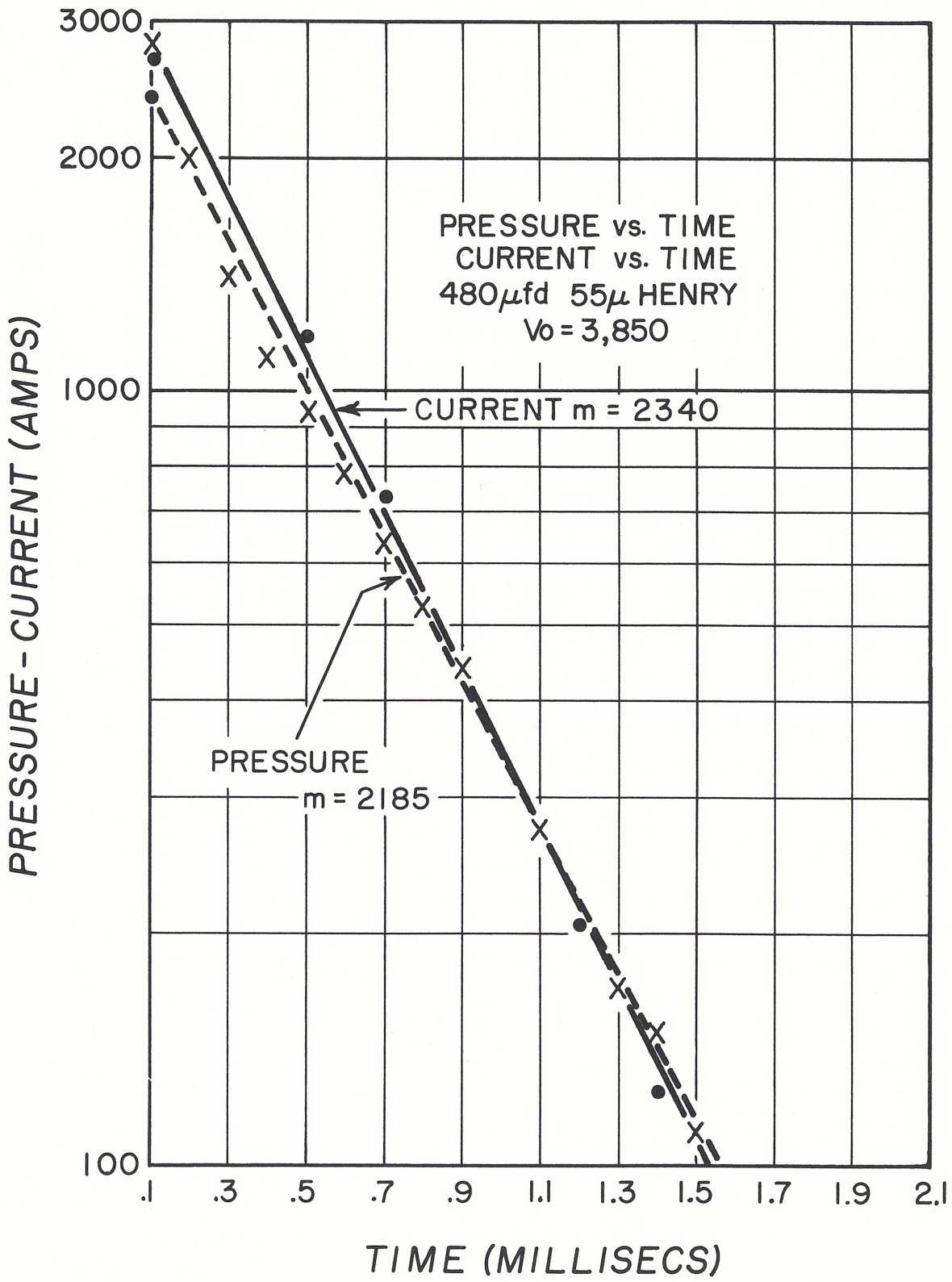
3000
2000
1000
100
PRESSURE vs. TIME
CURRENT vs. TIME
480μfd 55μ HENRY
Vo = 3,850
CURRENT m = 2340
PRESSURE
m = 2185
PRESSURE - CURRENT (AMPS)
.1
.3
.5
.7
.9
1.1
1.3
1.5
1.7
1.9
2.1
TIME (MILLISECS)

FIGURE 12b

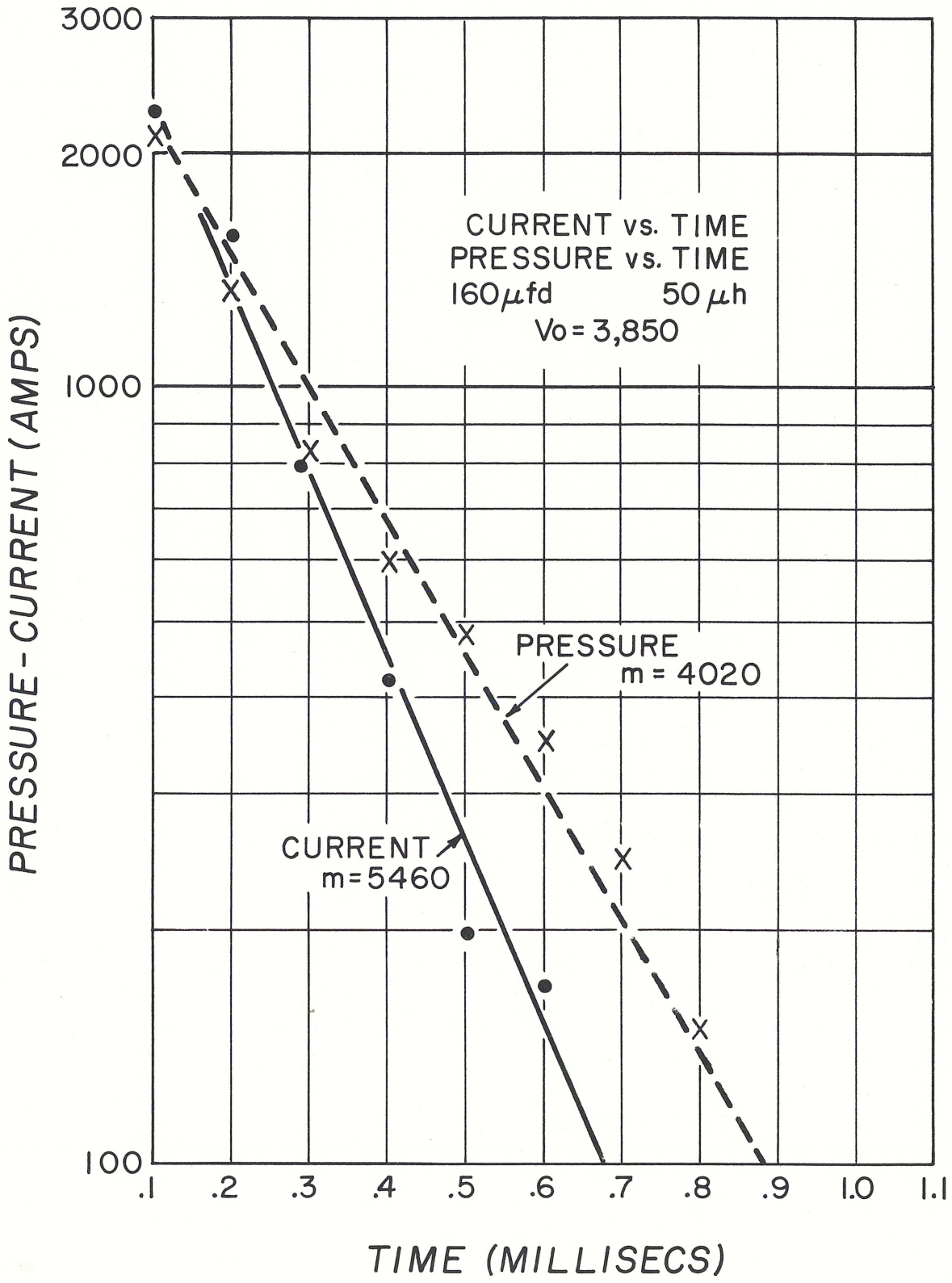
3000
2000
1000
100
.1
.2
.3
.4
.5
.6
.7
.8
.9
1.0
1.1
CURRENT vs. TIME
PRESSURE vs. TIME
160μfd 50 μh
Vo = 3,850
PRESSURE
m = 4020
CURRENT
m=5460
PRESSURE - CURRENT (AMPS)
TIME (MILLISECS)

FIGURE 12c

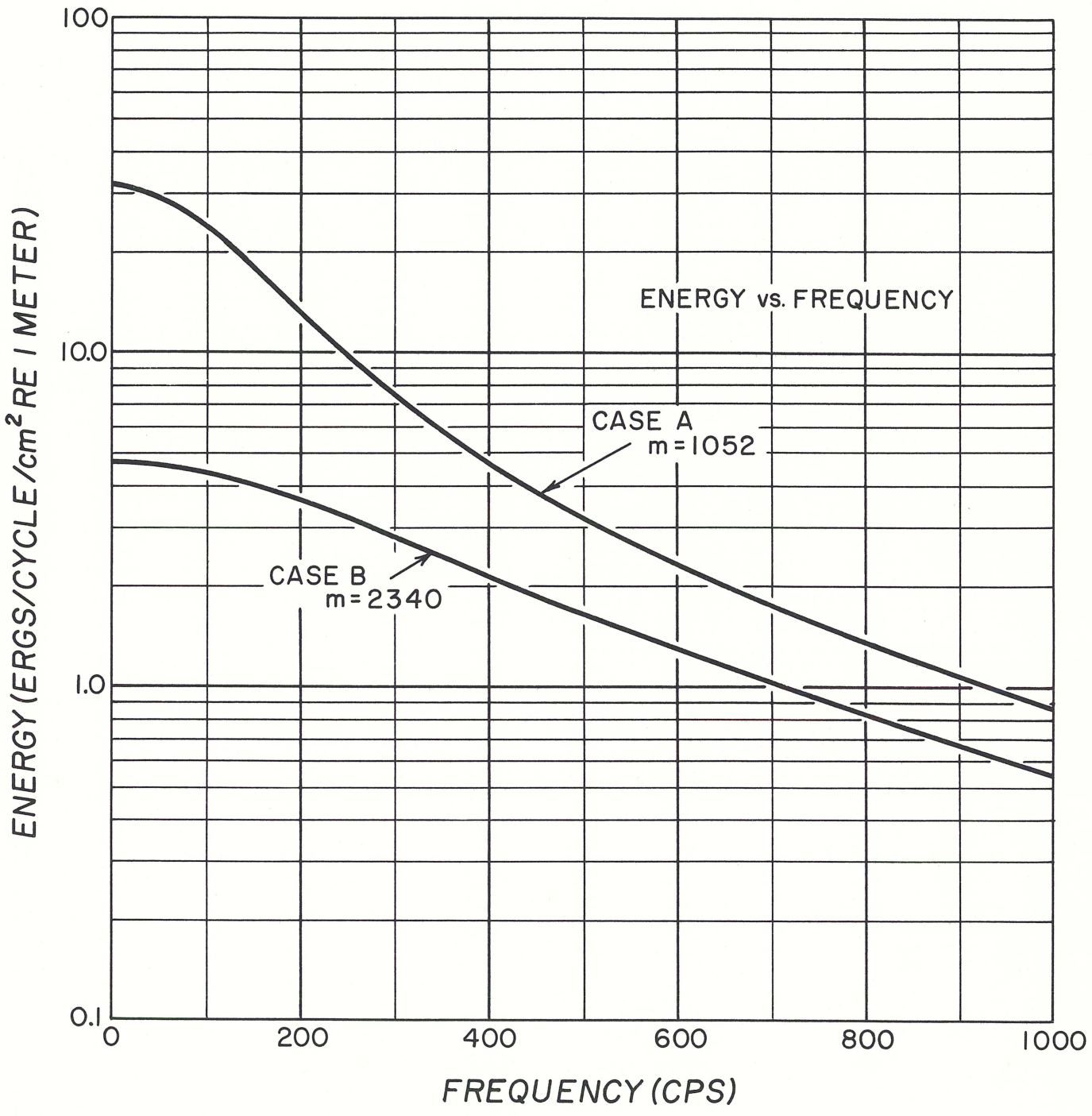
100
10.0
1.0
0.1
0
200
400
600
800
1000
ENERGY (ERGS/CYCLE/cm² RE 1 METER)
FREQUENCY (CPS)
ENERGY vs. FREQUENCY
CASE A
m = 1052
CASE B
m = 2340

FIGURE 13

Section I. SUMMARY

It is now possible to choose the electrical parameters of a sparker system so that a desired peak pressure and decay constant can be obtained with the corresponding energy spectrum. The restrictions on the above are a peak voltage of 11,000 volts and the use of the simple electrode system. Extrapolation to higher voltages is probably possible.

In choosing the parameters of the system, the inductance of the capacitors and switching system is the most difficult to determine. Using reasonable care in the geometry of the capacitor-switch connections the inductance can be kept below 0.5 microhenries.

The inductance, resistance, and capacitance of the discharge lines are readily obtained, and the resistance of the spark gap can be taken as 1.10 ohms.

Section J. ACKNOWLEDGEMENTS

The author wishes to express his thanks to the following people without whose help this project could not have reached completion: Dr. E. Hays, Mr. F. Birch, Mr. J. Riegel, Mr. S. T. Knott, Mr. W. Witzell, Mr. A. Nalwalk, and Mr. R. Nowak.

Section K. BIBLIOGRAPHY

1. The Underwater Spark: An Example of Gaseous Conduction at about 10,000 Atmosphere. Edward A. Mortin Engineering Research Institute, University of Michigan, #2048-12-F.

2. Collapse of a Transient Cavity in a Compressible Liquid. Hugh G. Flynn, March 1, 1957, Acoustic Research Laboratory, Harvard University, Cambridge, Massachusetts.

3. An Investigation of Underwater Spark. Warren Moon, June, 1958, Massachusetts Institute of Technology.

4. Underwater Spark and Blasting Caps as Sources of Sonic Energy, Deep Water Tests on Underwater Spark, First Interim Progress Report on Underwater Spark Acoustic Source Investigation Reports from Project No. 94-9426-05, R and D Department, Stromberg-Carlson.

5. An Experimental Study of the Collapse of a Spherical Cavity in Water. Robert H. Mellen, The Journal of the Acoustical Society of America, Vol. 28, No. 2, May, 1956.

6. Sound Speed and Absorption Studies of Marine Sediments by a Resonance Method, Part II. George Shumway, June, 1960, Geophysics, Vol. XXV, No. 3, p. 659.

7. I. T. T. Handbook of Radio and Electronics, 1960 Edition.

8. W. E. Witzell, S. T. Knott, and J. B. Hersey Research Group Sparker, Woods Hole Oceanographic Institution, 1953-54.

9. Edgerton, Germeshausen, and Grier Boomer power supplies and capacitors used as a storage unit.

DISTRIBUTION LIST
WHOI Ref. No. 62-12

	No. of copies
Bell Telephone Laboratories Whippany, New Jersey Attn: C. F. Weibush, Dept. 411	2
Chief, Bureau of Ships Department of the Navy Washington 25, D. C.	
Attn: Code 335	1
Code 341	1
Code 631	1
Code 689B	1
Bureau of Naval Weapons Department of the Navy Washington 25, D. C.	1
Mr. Murray H. Schaffer Bureau of Naval Weapons Department of the Navy Washington 25, D. C. Attn: RU-222	1
Hudson Laboratories 145 Palisade Street Dobbs Ferry, New York Attn: Dr. R. A. Frosch	1
U. S. Navy Hydrographic Office Washington 25, D. C. Attn: Hydrographer	2
Lamont Geological Observatory Torrey Cliff Palisades, New York Attn: Director	1
Office of Naval Research Department of the Navy Washington 25, D. C.	
Attn: Code 468	1
Code 416	1
Code 418	1
Code 466	2

	No. of copies
Defense Research Laboratory University of Texas Austin, Texas Attn: Dr. C. P. Boner, Director	1
Submarine Development Group TWO c/o Fleet Post Office New York, New York Attn: Commander	1
Department of Oceanography Texas A and M College College Station, Texas Attn: Director	1
Marine Laboratory University of Miami 1 Rickenbacker Causeway Virginia Key Miami 49, Florida Attn: Director	1
Narragansett Marine Laboratory University of Rhode Island Kingston, Rhode Island Attn: Director	1
U. S. Naval Ordnance Test Station Pasadena Annex 3202 East Foothill Boulevard Pasadena 8, California Attn: Library	1
U. S. Naval Postgraduate School Monterey, California Attn: Librarian	1
Office of Naval Research Project Officer U. S. Navy Sofar Station APO 856 c/o Postmaster, New York	1

	No. of copies
Office of Naval Research 495 Summer Street Boston, Massachusetts	1
U. S. Navy Mine Defense Laboratory Panama City, Florida Attn: Commanding Officer	1
Air Force Missile Test Center Technical Library, MU-135 Patrick Air Force Base, Florida	1
U. S. Navy Research Laboratory Washington, D. C.	
Attn: Captain Krapf	1
Dr. R. M. Page	1
Code 2021	1
Code 5500	1
Code 5510	1
U. S. Navy Underwater Sound Laboratory Fort Trumbull New London, Connecticut	
Attn: Director	3
Captain H. E. Ruble, USN	1
Dr. W. Horton	1
U. S. Naval Ordnance Laboratory White Oak, Silver Spring Maryland	
Attn: Captain M. A. Peterson, USN	1
Dr. G. K. Hartmann	1
David Taylor Model Basin Washington 25, D. C.	
Attn: Commanding Officer and Director (Code 560)	1
Radm. E. A. Wright, USN	1
Dr. K. E. Schoenherr	1
Daystrom Electric Division of Daystrom, Inc. 753 Main Street Poughkeepsie, New York	1

	No. of copies
Applied Physics Laboratory University of Washington 1013 East 40th Street Seattle 5, Washington Attn: Dr. J. B. Henderson	1
Commander U. S. Naval Ordnance Test Station China Lake, California Attn: Technical Director	1
Commander (Code 753) U. S. Naval Ordnance Test Station China Lake, California Attn: Technical Library	1
U. S. Naval Air Development Center Johnsville, Pennsylvania Attn: Director Dr. Harry Krutter	 1 1
Force ASW Officer Commander, Submarine Force U. S. Pacific Fleet c/o Fleet Post Office San Francisco, California	1
Anti-Submarine Defense Force U. S. Atlantic Fleet U. S. Naval Base Norfolk 11, Virginia	1
National Academy of Sciences National Research Council 2101 Constitution Avenue Washington, D. C. Attn: Mr. James H. Probus	1
Commanding Officer U. S. Naval Ordnance Laboratory White Oak, Silver Spring Maryland Attn: A. T. Jaques (RA)	1

	No. of copies
U. S. Naval Underwater Ordnance Station Newport, Rhode Island	
Attn: Commanding Officer	1
Dr. G. G. Gould	1
ONR Liaison Officer Woods Hole Oceanographic Institution Woods Hole, Massachusetts	2
Department of Geology University of Wisconsin Madison 6, Wisconsin Attn: Dr. G. P. Woollard	1
Fluid and Solid Mechanics Laboratory Institute of Science and Technology Post Office Box 618 Ann Arbor, Michigan Attn: Mr. John W. Wescott	1
Ordnance Research Laboratory University Park, Pennsylvania	
Attn: Development Contract Administrator	1
Dr. V. Albers	1
ASW Tactical School U. S. Atlantic Fleet Norfolk, Virginia Attn: Commanding Officer and Director	1
U. S. Navy Electronics Laboratory San Diego 52, California	
Attn: Commanding Officer and Director	1
Captain J. M. Phelps, USN	1
Dr. F. N. D. Kurie	1
Marine Physical Laboratory of the Scripps Institution of Oceanography San Diego 52, California Attn: Dr. F. N. Spiess, Director	1
Anti-Submarine Warfare Research Center La Spezia, Italy	1

	No. of copies
Destroyer Development Group TWO c/o Fleet Post Office New York, New York Attn: Commander	1
Destroyer Flottila THREE c/o Fleet Post Office San Francisco, California Attn: Commander	1
Anti-Submarine Defense Force U. S. Pacific Fleet Fleet Post Office San Francisco, California Attn: Commanding Officer	1
Institute for Defense Analyses Communications Research Division Von Neumann Hall Princeton, New Jersey	1
Pacific Oceanographic Group Nanaimo, British Columbia	1
Grumman Aircraft Engineering Corp. Bethpage, L. I., New York	1
Armed Services Technical Information Agency Arlington Hall Station Arlington 12, Virginia	10
Chief of Naval Operations Op-07T Washington 25, D. C.	1
Chief of Naval Operations (OpO3EG) Department of the Navy Washington 25, D. C. Attn: Mr. D. D. Bourland	1

	No. of copies
Seyir ve Hidrografi Dairesi Cubuklu-Istanbul, Turkey Via: ONR Branch Office London	1
National Institute of Oceanography Wormley Godalming, Surrey, England Attn: Library	1

Woods Hole Oceanographic Institution
Reference No. 62-12

Predicting Sonic Pulse Shapes of Underwater Spark Discharges, (U), by David D. Caulfield, 16 p, 13 fig., March 1962.

Unclassified

Measurements of the acoustic pressure of spark discharges were made at a shallow depth (10 feet) for various voltages, stored energies, inductances and capacitances of the system, and electrode areas. The voltages ranged from 1500V to 11 KV, and the energy storing capacitances from 8 to 800 ufd. In this range the peak pressure observed was proportional to peak current and the decay constant of the pressure-time curve was essentially the same as the electrical discharge decay constant.

1. Sound Transmission
2. Seismic Profiling
3. Underwater Spark Phenomena
4. High Energy Sources

This card is UNCLASSIFIED

Woods Hole Oceanographic Institution
Reference No. 62-12

Predicting Sonic Pulse Shapes of Underwater Spark Discharges, (U), by David D. Caulfield, 16 p, 13 fig., March 1962.

Unclassified

Measurements of the acoustic pressure of spark discharges were made at a shallow depth (10 feet) for various voltages, stored energies, inductances and capacitances of the system, and electrode areas. The voltages ranged from 1500V to 11 KV, and the energy storing capacitances from 8 to 800 ufd. In this range the peak pressure observed was proportional to peak current and the decay constant of the pressure-time curve was essentially the same as the electrical discharge decay constant.

1. Sound Transmission
2. Seismic Profiling
3. Underwater Spark Phenomena
4. High Energy Sources

This card is UNCLASSIFIED

Woods Hole Oceanographic Institution
Reference No. 62-12

Predicting Sonic Pulse Shapes of Underwater Spark Discharges, (U), by David D. Caulfield, 16 p, 13 fig., March 1962.

Unclassified

Measurements of the acoustic pressure of spark discharges were made at a shallow depth (10 feet) for various voltages, stored energies, inductances and capacitances of the system, and electrode areas. The voltages ranged from 1500V to 11 KV, and the energy storing capacitances from 8 to 800 ufd. In this range the peak pressure observed was proportional to peak current and the decay constant of the pressure-time curve was essentially the same as the electrical discharge decay constant.

1. Sound Transmission
2. Seismic Profiling
3. Underwater Spark Phenomena
4. High Energy Sources

This card is UNCLASSIFIED

Woods Hole Oceanographic Institution
Reference No. 62-12

Predicting Sonic Pulse Shapes of Underwater Spark Discharges, (U), by David D. Caulfield, 16 p, 13 fig., March 1962.

Unclassified

Measurements of the acoustic pressure of spark discharges were made at a shallow depth (10 feet) for various voltages, stored energies, inductances and capacitances of the system, and electrode areas. The voltages ranged from 1500V to 11 KV, and the energy storing capacitances from 8 to 800 ufd. In this range the peak pressure observed was proportional to peak current and the decay constant of the pressure-time curve was essentially the same as the electrical discharge decay constant.

1. Sound Transmission
2. Seismic Profiling
3. Underwater Spark Phenomena
4. High Energy Sources

This card is UNCLASSIFIED